Journal of Engineering Physics and Thermophysics, Vol. 76, No. 1, 2003

RHEOLOGICAL BEHAVIOR AND STRENGTH OF COMPOSITE SYSTEMS OF THE TYPE "ALUMINUM OR ITS ALLOY (POLYMER)–OXIDE CERAMICS–CHROMIUM CARBIDE"

M. V. Kireitsev

UDC 621.763:539.4

Rheological methods are proposed and on their basis methods for calculating strength and load characteristics of composite systems of the type "aluminum or its alloy (polymer)–oxide ceramics–chromium carbide" have been developed. The rheological behavior of systems under their local loading has been considered. The results of the comparison between the calculated and experimental results have confirmed the adequacy of the developed models and methods. Allowable specific contact pressures of composite systems have been established.

Introduction. Creation on the surface of machine elements of coatings with improved rheological and strength characteristics is one of the most effective and economical techniques widely used in universal practice [1–8].

Oxide ceramics is a popular engineering ceramics since it features a high microhardness (up to 22 GPa), wear resistance, and thermostability (900^{o}C or more) with a relatively cheap (about 2–5 \$/dm^2) and simple technology of its production. Adhesion (up to 300–450 MPa) between the oxide ceramics layer and the aluminum substrate increases the service life of oxide–ceramic composite coatings.

Analysis of the data of [2–8] has shown that the porosity of oxide ceramics influences its strength and wear resistance. Pores and other defects are concentrators of stresses. As a rule, these defects of metal ceramics are difficult to correct by means of many traditional kinds of mechanical treatment. Therefore, it is necessary to develop and investigate new designs of bearing assemblies, friction pairs, and sliding bearings designed with the use of composite systems based on oxide ceramics that increase their strength and load characteristics.

At the Institute of Reliability and Longevity of Machines of the National Academy of Sciences of Belarus, a number of designs of dynamically loaded bearing assemblies and sliding bearings with improved strength and vibration–proof characteristics designed with the use of composite systems of the type of "steel base–thermoplastic polymer–aluminum alloy–oxide ceramics," "aluminum alloy–oxide ceramics," and "aluminum alloy–oxide ceramics–pyrolytic chromium carbide" have been designed and investigated [2–4, 9–15].

Many researchers [16–20] have noted very low strength characteristics of oxide ceramic layers on aluminum substrates under the action of localized dynamic and static loads, which considerably limits the fields of their use in bearings and assemblies. Other authors [2–4, 11–13] have established a high serviceability and improved strength characteristics of oxide ceramics in operating in friction pairs. Despite the large number of publications on this problem [2–20], there are practically no literature data on the load-carrying capacity and rheological behavior of assemblies designed with the use of composite systems based on oxide ceramics placed on aluminum–alloy bases and on the influence of the composition, the structure, and the physicomechanical properties of layers of composite systems on the serviceability of assemblies.

The limitations of the existing methods of forecasting the strength and load characteristics of composite systems make it impossible to take into account a number of important physicomechanical characteristics of their layers as well as the influence of a soft aluminum or polymeric substrate on the strength of the system as a whole. For composite oxide–ceramics–based systems, experimentally substantiated rheological models taking into account their physicomechanical and strength characteristics are absent.

Theoretical Approach. With the complexity of the multilayer composite system taken into account, the following requirements placed upon a rheological model describing its deformed–stressed state have been formulated: a)

Institute of Reliability and Longevity of Machines, National Academy of Sciences of Belarus, Minsk, Belarus; email: indmash@yandex.ru. Translated from Inzhenerno-Fizicheskii Zhurnal, Vol. 76, No. 1, pp. 151–158, January–February, 2003. Original article submitted August 10, 2002.

1062-0125/03/7601-0179\$25.00

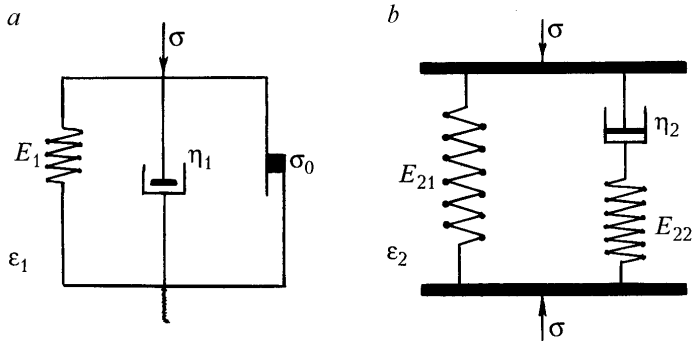

Fig. 1. Rheological models: a) elastoviscoplastic model of the composite system; b) parallel connection of the Maxwell model and the elastic element.

irreversible deformations become plastic and develop only if a certain critical value of the yield strength is exceeded; b) deformations at a constant stress smaller than the yield strength gradually grow to reach a finite value; c) under multiple loadings there occurs an accumulation of plastic deformations; d) the deformation–time (ε–τ) curve at a constant stress has a linear portion; e) upon unloading, retardation of deformations (elastic recovery) is observed; f) under constant deformation of the composite system's polymeric layers the stresses relax.

Thus, it is expedient to represent the proposed composite systems in the form of rheological models (Fig. 1) or their series connection. The rheological behavior of systems under localized loading can be considered by comparing the calculated and experimental data.

At a series connection of models the total deformation of the system being considered is expressed as

$$\varepsilon = \varepsilon_1 + \varepsilon_2 . \tag{1}$$

If $\sigma > \sigma_0$, then the rheological behavior of the first part of the model (Fig. 1a) can be given by the rheological equation

$$\sigma = \sigma_0 + E_1\varepsilon_1 + \eta_1 \frac{d\varepsilon_1}{dt} . \tag{2}$$

For the second part of the model (Fig. 1b), the differential equation can be written in the following form:

$$\frac{d\sigma}{dt} + \frac{E_{22}}{\eta_2}\sigma = (E_{21} + E_{22})\frac{d\varepsilon_2}{dt} + \frac{E_{21}E_{22}}{\eta_2}\varepsilon_2 . \tag{3}$$

With an arbitrary loading law the structural rheological equation of a composite system consisting of a series connection of models 1 and 2 will be described by the expression

$$\frac{\eta_1}{E_{22}}\frac{d^2\sigma}{dt^2} + \left(\frac{E_1}{E_{22}} + \frac{\eta_1}{\eta_2} + \beta\right)\frac{d\sigma}{dt} + \frac{E_1 + E_{21}}{\eta_2}\sigma - \frac{E_{21}}{\eta_2}\sigma_0 = \beta\eta_1\frac{d^2\varepsilon}{dt^2} + \left(\frac{\eta_1}{\eta_2}E_{21} + \beta E_1\right)\frac{d\varepsilon}{dt} + \frac{E_1E_{21}}{\eta_2}\varepsilon . \tag{4}$$

Let us consider the basic rheological equations describing the behavior and strength characteristics of a composite system or its layers for various types and loading conditions.

Deformation of a model composite medium at σ = const:

1. At $\sigma \le \sigma_0$ and $\varepsilon_1 = 0$ the general solution of Eq. (3) is of the form

$$\varepsilon(t) = \frac{\sigma}{E_{21}}\left(1 - \frac{1}{\beta}\exp(-t/t_{unl2})\right), \tag{5}$$

where $t_{unl2} = \beta\eta_2/E_{21}$ and $\beta = 1 + E_{21}/E_{22}$.

At an infinitely sustained loading the finite deformation is equal to σ/E_{21} and the loading law can be given by

$$\sigma(t) = (E_{21} + E_{22})\,\varepsilon_2(t) - \frac{E_{22}}{t_{unl2}}\int_0^t \varepsilon_2(\tau)\exp[(-t+\tau)/t_{unl2}]\,d\tau + C\exp(-t/t_{unl2}). \quad (6)$$

In expression (6), the integration constant C is determined by the initial condition. If $\sigma(0) = 0$ and $\varepsilon_2(0) = 0$, then $C = 0$.

2. At $\sigma > \sigma_0$ and $\varepsilon_1(0) = 0$ the total deformation of the medium at a fixed loading is described by the following relation:

$$\varepsilon(t) = \frac{\sigma - \sigma_0}{E_1}(1 - \exp(-t/t_{unl1})) + \frac{\sigma}{E_{21}}\left(1 - \frac{1}{\beta}\exp(-t/t_{unl2})\right). \quad (7)$$

Unloading after loading:

1. At $\sigma_1 \le \sigma_0$ the deformations of the first and second elements of the mechanical model at time t_1 are equal, respectively, to $\varepsilon_1(t_1) = 0$ and

$$\varepsilon_2(t_1) = \frac{\sigma_1}{E_{21}}\left(1 - \frac{1}{\beta}\exp(-t_1/t_{unl2})\right). \quad (8)$$

The unloading process under the initial condition (8) is defined by the expression

$$\varepsilon_2(t) = \frac{\sigma_1}{\beta E_{21}}(1 - \exp(-t_1/t_{unl}2))\exp[-(t-t_1)/t_{unl2}]. \quad (9)$$

2. If $\sigma > \sigma_0$, then the total deformation at unloading is found from the expression

$$\varepsilon(t) = \frac{\sigma_0}{E_1} + \frac{\sigma_1 - \sigma_0}{E_1}(1 - \exp(-t_1/t_{unl1}))\exp[-(t-t_1)/t_{unl1}] + \frac{\sigma_1}{\beta E_{21}}(1 - \exp(-t_1/t_{unl2}))\exp[-(t-t_1)/t_{unl2}], \quad (10)$$

where $t_{unl1} = \eta_1/E_1$.

Loading at a constant deformation:

1. If $\varepsilon_0(E_{21} + E_{22}) \le \sigma_0$, then at $\varepsilon_1 = 0$ and $\varepsilon_2 = \varepsilon_0 = \text{const}$ the loading law is expressed by the function

$$\sigma(t) = \varepsilon_0 E_{22}\left(\frac{E_{21}}{E_{22}} + \exp(-t/t_{unl})\right), \quad (11)$$

and at an infinitely sustained loading function (11) will be of the following form:

$$\sigma(t \to \infty) = \varepsilon_0 E_{21}.$$

2. If $\varepsilon_0(E_{21} + E_{22}) > \sigma_0$ and $\varepsilon_1 = 0$, and $\varepsilon_2 = \varepsilon_0 = \text{const}$, then the sought loading law can be given by the expression

$$\sigma(t) = C_{11}\exp[-(\varphi + D)\,t/2] + C_{12}\exp[-(\varphi - D)\,t/2] + S/\psi, \quad (12)$$

where the conventionally taken coefficients are expressed as

$$\varphi = \frac{E_{22}}{\eta_1}\left(\frac{E_1}{E_{22}} + \frac{\eta_1}{\eta_2} + \beta\right); \quad \psi = \frac{E_{22}}{\eta_1\eta_2}(E_1 + E_{21}); \quad S = \frac{\sigma_0 + \varepsilon_0 E_1}{1 + E_1/E_{21}};$$

TABLE 1. Parameters of the Composite Systems

Parameters	$Al–Al_2O_3$	$Al–Al_2O_3–CrC$	Steel–Polymer–$Al–Al_2O_3$	Steel–$Al–Al_2O_3–CrC$	Steel–CrC
Microhardness, GPa	12–18	14–22	8–12	8	10–12
Collapsing load (for a ball of diameter no more than 7.938 mm), N	200	500	100	180	110
Specific contact pressure, no more than, GPa	1.8	3.0	1.5	2.5	2.1

$$D = \sqrt{\varphi^2 - 4\psi}\ ;\quad C_{11} = \frac{R_2 - R_1(\varphi - D)}{2D}\ ;\quad C_{12} = \frac{R_1(\varphi + D) - R_2}{2D}\ .$$

Thus, the proposed rheological models make it possible to establish a correlation between the structural–mechanical properties (elasticity, viscosity, plasticity), the physicochemical structure, and the composite system design, evaluate their strength and load characteristics at the stage of designing bearing assemblies and sliding bearings, and increase the accuracy of predicting the stressed-deformation state of coatings under different conditions of their loading. The adequacy of the proposed rheological models should be verified by experiment.

Experimental Data. The test specimens had the form of 2.5 × 10.0 × 0.5 cm plates on which the following composite systems were formed: (1) "aluminum oxide–D16 aluminum alloy" ($Al_2O_3–Al$); (2) "pyrolytic chrome carbide–steel base" (CrC–steel 45); (3) chromium carbide–aluminum oxide–D16 aluminum alloy ($CrC–Al_2O_3–Al$); and (4) "steel substrate–polymer–aluminum alloy–oxide ceramics."

The composite system "steel base–polymer–aluminum alloy–oxide ceramics" was formed on a steel billet (steel 45) 31.2 mm in diameter with projections and hollows having a profile depth of 500 μm and a 2.5 × 2.5 μm section. Then, on the above surface, using a plant of gas-thermal spraying of low-melting materials, a PA6-21G polyamide layer with an elastic modulus of 4 GPa and a thickness of 420 μm was formed [10, 13].

After that, on the polymer surface, by means of gas-thermal spraying, a 3.4-mm-thick aluminum layer was formed by aluminum particles with a mean size of 70 μm at a temperature of 1200°C. In so doing, the aluminum layer surface contacting the polymer forms a complementary polymeric surface. Then a 200-μm-thick layer of oxide ceramics was formed as a result of the transformation of the surface aluminum layer caused by the microarc treatment.

For the composite systems "aluminum oxide–aluminum alloy" and "pyrolytic chromium carbide–aluminum oxide–aluminum alloy," an oxide ceramic layer of thickness 100–300 μm and microhardness 15 to 19 GPa was formed out by the method of microarc anode-cathode treatment (MAT) in an ecologically safe electrolyte based on a solution of Na_2SiO_3 liquid glass (State Standard 13078-67) with a modulus of 3 to 3.4 of density 1.4 to 1.5 g/cm^3 — 6 g/liter — and of pure KOH potassium hydroxide (State Standard 9285-78) — 3 g/liter in distilled water.

The MAT method makes it possible to form a high-strength oxide-ceramics layer on the aluminum alloy surface, thereby retaining the size and shape of the surfaces being treated. Microarc oxidation was carried out with the use of a pulsed power source with controlled frequency and voltage. The porosity and structure of oxide ceramics are controlled by regulating the current densities, increasing them at individual treatment stages up to 30 to 40 A/dm^2 depending on the element material and the required coating thickness.

A pyrolytic chromium carbide layer with a thickness of 10 to 15 μm and a microhardness of 10 to 12 GPa was applied to the oxide-ceramic base by the method of pyrolysis of the "Barkhos" organochromium liquid [13] at a vapor pressure in the chamber from 7 to 9 Pa. In the process of deposition of chrome carbide particles, the base was maintained at a temperature between 420 and 430°C. A pyrolytic chromium carbide layer of thickness above 20 μm has stronger internal stresses, leading to its destruction. This process ensures penetration of chrome carbide into the cracks and pores. The parameters of the layers of composite systems and their load characteristics are given in Table 1.

Evaluation of the load-carrying capacity of the composite systems was carried out on a test bed incorporating a uniform loading device, a load indicator unit, and an indentor fixing device. The behavior of the proposed rheological models was considered with the example of pressing an indentor of diameter 7.938 mm into the test specimen. Then the decrease in the contact force was registered and the size of the obtained indentation was determined. The loading rate was 10 N/sec or higher, and the indentation load was varied from 1 to 1000 N.

The sought law of loading of the composite system given in Fig. 1a is defined by Eq. (2), which, after its integration on the assumption that the time dependence of the deformation is linear, will be of the form

$$\sigma(t) = \sigma_0 + E_1\varepsilon_0 + \eta_1\dot{\varepsilon}(0) + E_1\varepsilon(0)\,t\,. \tag{13}$$

The sought law of loading of the multi-element rheological system given in Fig. 1b is defined by Eq. (3), which, after its integration on the assumption that the time dependence of the deformation has the form of the function $\varepsilon(t) = \varepsilon_0 + kt$ can be given in the following form:

$$\sigma(t) = (\eta_2 k - E_{22}\varepsilon_0)\,(1 - \exp(-t/t_{\text{unl}}) + E_{21}kt + \beta E_{22}\varepsilon_0\,. \tag{14}$$

It should be noted that there exist more complicated laws of change in the deformation (for example, quadratic ones), which, in combination with rheological equations, can describe in more detail the stressed-deformation state as opposed to the above equations (13) and (14). Therefore, in a number of cases, to describe the rheological behavior of the system's elements (Fig. 1), it is more rational to integrate on the assumption that the time dependence of the deformation is quadratic. Then the sought loading law of the composite system as a whole at a series connection of models 1 and 2 will yield an analytical solution to the following equation:

$$\sigma(t) = \exp\left(-\frac{A}{2}\Delta t\right)\left[\sinh\left(\frac{AD}{2}\Delta t\right)\frac{F-M}{K} + x\cosh\frac{AD}{2}\Delta t\right] + \sigma_0 - F\,, \tag{15}$$

where the coefficients taking into account the structural-mechanical properties of the system are given by the relations

$$x - y = \sigma_0 - \frac{S_0^*}{B} + \frac{AS_1^* - 2S_2^*}{B^2} - \frac{2A^2S_2^*}{B^3} - \frac{2\sigma_0}{A} + \frac{2S_1^*}{AB}\,; \quad A = \frac{E_{22}}{\eta_1}\left(\frac{E_1}{E_{22}} + \frac{\eta_1}{\eta_2} + \beta\right); \qquad B = \frac{(E_1 + E_{22})/E_{22}}{\eta_1\eta_2}\,;$$

$$K = \sqrt{1 - 4\frac{\eta_1}{\eta_2}\frac{(E_1 + E_{21})/E_{22}}{(E_1/E_{22} + \eta_1/\eta_2 + \beta)^2}}\,; \qquad S_0 = \frac{E_{21}E_{22}}{\eta_1\eta_2}\sigma_0 + \beta E_{22}k_2 + \frac{E_{22}}{\eta_1}\left(\frac{\eta_1}{\eta_2}E_{21} + \beta E_1\right)k_1\,;$$

$$S_1 = \frac{E_{22}}{\eta_1\eta_2}\left(\frac{\eta_1}{\eta_2}E_{21} + \beta E_1\right)k_2 + \frac{E_1E_{21}E_{22}}{\eta_1\eta_2}\varepsilon_0\,; \qquad S_{21} = \frac{E_1E_{21}E_{22}}{\eta_1\eta_2}\frac{1}{2}k_2\,.$$

While the qualitative solution of the multiparametric equation (15) is relatively easy to find, its qualitative expression and practical application entail difficulties; therefore, Eq. (15) was not used in the experiment.

It is customary to assume [1, 18–20] that in pressing a spherical indenter into an isotropic half-space, the deformation value equivalent to the deformed state of the material under uniform compression is proportional to the ratio between the indentation diameter and the indenter radius in the form $\varepsilon(t) = 2kd(t)/R$. Expressing the indentation parameter in terms of the impression depth α_{ind} and the radius of curvature R, we obtain $d(t) = 2\sqrt{R\alpha_{\text{ind}}(t)}$. Then the loading law with regard for the conditions for localized loading modeling the Hertzian contact [1, 17–20] can be given in the form

$$P(t) = \sigma(t)\left[\pi RVt + \frac{\pi d^2(t)}{4}\right]. \tag{16}$$

The deformation dependences of the stress (13)–(14) and the indentation-depth dependences of the contact force (16) contain elasticity and viscosity parameters E_{21}, E_{22}, and η_2 characterizing the properties of a polymer material. Here E_{21} and η_2/E_{22} can be found by experiment or in [16].

Figure 2 shows the relations between the load applied to the indenter and the deformation value (impression depth in the coating) obtained by expressions (13)–(16). As follows from Fig. 2, the agreement between the experimental and calculated data for both composite systems is quite satisfactory if one takes into account the assumptions made in using the formulas.

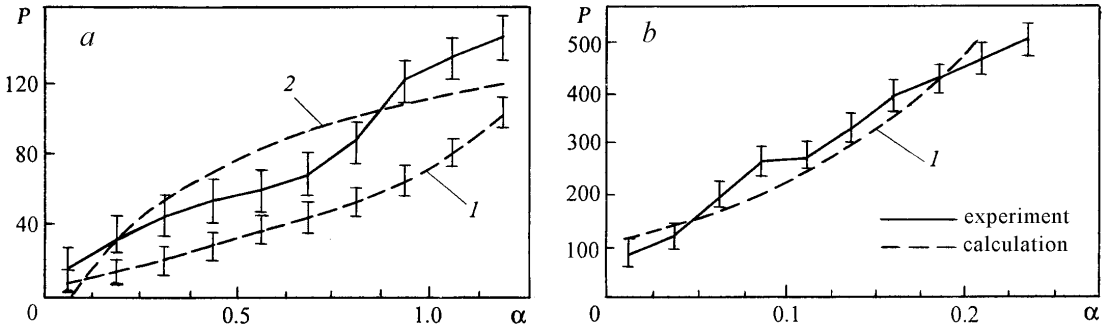

Fig. 2. Load characteristics of multi-element rheological systems: a) "oxide ceramics–aluminum alloy–viscoelastic material–steel base"; b) "chromium carbide–oxide ceramics–aluminum or its alloy" (1 and 2 correspond to models 1 and 2). P, N; α, mm.

TABLE 2. Parameters of the Load-Carrying Capacity of the Composite System of the Type "Aluminum or Its Alloy–Oxide Ceramics–Chromium Carbide"

Load P, N	Contact pressure P_0, MPa		Compression stress σ_y, MPa		Tensile stress σ_x, MPa		Depth of shear stress propagation, μm	
	I	II	I	II	I	II	I	II
100	2654	1674	826	522	393	249	64.4	81.2
200	3343	2108	1039	656	494	313	81.2	107
300	3826	2412	1189	751	565	358	92.9	122
400	4211	2654	1308	826	621	393	107	133
500	4535	2859	1409	889	669	423	115	143
1000	5713	3601	1774	1119	842	532	143	179

Note: I, D = 3.938; II, D = 7.938.

In a number of cases, to describe the rheological behavior of a composite system in which polymer layers with a thickness much greater (by a factor of 5–10 or more) than the thickness of metal-ceramic layers prevail, it is expedient to use a rheological model consisting of a parallel-connected element and a Maxwell model. In this case, the elastic polymer component of the composite system largely determines its rheological behavior and load-carrying capacity. Plastic deformations and destruction of the composite occur under the conditions of large elastic deformations of the polymer layers. The elastoviscoplastic rheological model will be adequate in calculating the rheological behavior of composite systems of the type of "pyrolytic chromium carbide–aluminum oxide–aluminum alloy" and "oxide ceramics–aluminum alloy–polymer (of thickness up to 500 μm)–steel base."

In general, the developed method for calculating and predicting the strength and load characteristics can be used for composite systems based on oxide ceramics.

The investigations of the destruction of the layers of systems were based on the measurement of their deformation parameters. Depending on the loading force, on the specimen surface a dent is obtained. After each loading cycle the radius of the obtained dent was measured with the aid of an optical microscope by determining the size of the reflected light spot from the contact region. The results of the calculation of the load characteristics are given in Table 2 by means of the points of the Hertz theory [1]. The dynamics of the change in the specific contact pressure of the investigated composite systems of the type "aluminum alloy–oxide ceramics–chromium carbide" and "steel base–polymer–aluminum alloy–oxide ceramics" is given in Fig. 3.

The preliminary experimental data [13, 14] indicate that composite systems of the type "aluminum oxide–aluminum alloy" and "pyrolytic chromium carbide–steel base" do not provide an improved load-carrying capacity and strength characteristics, failing under localized loads of about 100 N per spherical indenter of diameter 7.938 mm.

As the analysis of the data has shown, under a localized loading the relative admissible specific contact pressures for the "aluminum alloy–oxide ceramics–chromium carbide" system are equal to 3 GPa and for the composite

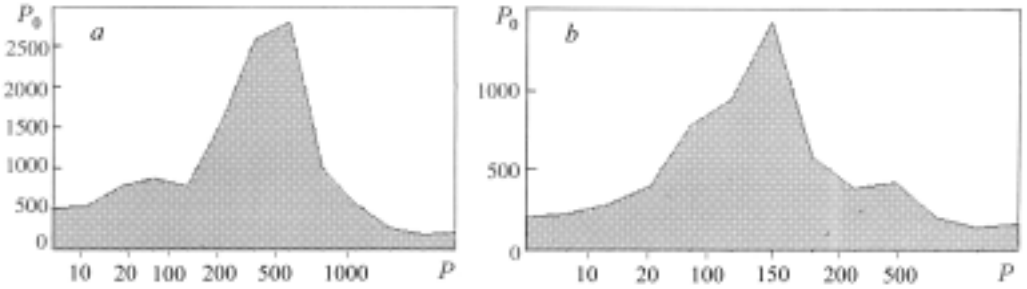

Fig. 3. Dynamics of change in the specific contact pressure of composite systems: a) "aluminum or its alloy–oxide ceramics–chromium carbide"; b) "steel base–polymer–aluminum or its alloy–oxide ceramics." P_0, MPa; P, N.

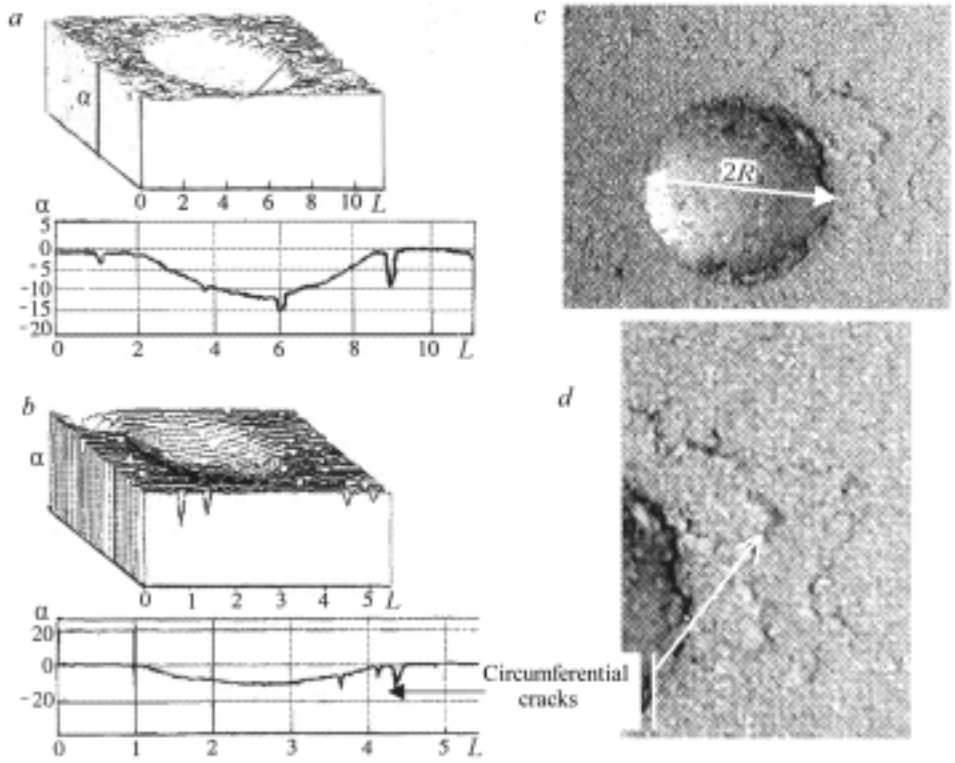

Fig. 4. Deformations and destruction of the composite system "aluminum alloy–oxide ceramics–chromium carbide": a and c) 3-D and 2-D views of the dent, respectively; b and d) 3-D and 2-D (×1000) view of the cracks. $L \cdot 10^{-4}$, m.

system including polymer layers — from 1.0 to 1.5 GPa. When the revealed technological regimes of pyrolysis are provided, the coating from chromium carbide applied to an oxide ceramic base features a higher adhesion to oxide ceramics (up to 250 MPa), which is due to the presence of chemically interlinked compounds in the structure of the layer, such as oxygen and aluminum elements.

The investigations of the microstructures of the composite system layers have shown that the chromium carbide particles fill the surface microdefects, pores, and microcracks of oxide ceramics, thus increasing the strength and load-carrying characteristics of the composite. The filling of the pores and defects of oxide ceramics with a chromium carbide layer makes it possible to effectively prevent the appearance and propagation of cracks in the composite under its localized loading. The composite microhardness, especially in the surface layers at the oxide–carbide interface, increases up to 15 GPa.

As the calculations and load tests at above 500 N have shown, the stresses arising in the indenter–surface contact zone penetrate to a considerable depth (up to 200 μm), reaching their maximum concentration in the zones of

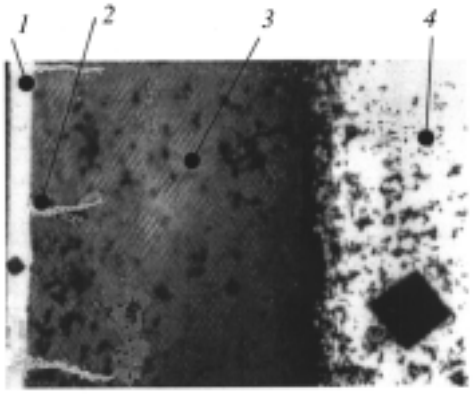

Fig. 5. Photograph of the microstructure of the "pyrolytic chromium carbide–oxide ceramics–aluminum alloy" system: 1) chromium carbide; 2) cracks of the surface layer of oxide ceramics filled with chromium carbide; 3) oxide ceramics; 4) base (aluminum alloy).

localization of solid crystals of aluminum oxide and in the zones of a higher porosity and a larger number of microdefects. As a result, this promotes cracking and a considerable deformation of the composite system (Fig. 4).

The composite system of the type of "aluminum or its alloy–oxide ceramics–chromium carbide" has improved strength characteristics. The specific contact pressures for this system reach 3 GPa under loads of up to 500 N and at an indenter diameter of 7.938 mm.

Because of the small thickness, the chromium carbide layer has an insignificant level of internal and residual stresses associated with the technology of its formation. The penetration of chromium carbide particles into the pores and cracks to a depth of 25–60% from the layer thickness (shown in Fig. 5) reinforces the oxide ceramic surface, impeding the crack propagation and preventing local destruction of the layer under the action of contact pressures to provide better strength characteristics of the composite under the action of intense loads compared to the existing analogs.

Comparison of the calculated data obtained with the use of the proposed rheological models with the experimental results has shown that in the region of relatively low contact pressures of 1 to 3 GPa they practically do not disagree with one another. A further increase in the load leads to failure of the composite system. Deformation is largely due to the radial extension of the contact region under the indenter, leading to the formation of circumferential and cone-shaped cracks in the coating (Fig. 4c, d). A plastic flow equalizes the pressures and accompanying stresses in the contact region, slightly affecting the base material.

In general, for the developed composite systems, the base hardness insignificantly increases the loading characteristics of the whole composite. The depth of indenter penetration into the coating depends on the oxide–ceramics thickness, and its layers thereby resist failure until a critical contact pressure (up to 1.5–2 Hz) is reached, leading to a destruction (crack) and forming a cracking region (e.g., in the form of a cone), a concentric or circular region.

An increase in the contact pressure and a superposition of the field of tensile and compression stresses on one another lead, in a number of cases, to circumferential macrocracks, coating detachment, and chippings, especially in the region of pores and microdefects concentrating stresses. The most rational thicknesses of the oxide-ceramic layer are 50 to 300 μm and of the chromium carbide layer — 5 to 50 μm.

We have developed, manufactured, and subjected to service tests at the State Industrial Association "Khimvolokno" in Grodno development and production prototypes of sliding bearings with composite coatings on working surfaces, which have demonstrated a prolonged service life, providing trouble-free operation for 18,000 hours.

CONCLUSIONS

In the present paper, we propose and have experimentally substantiated approaches using rheological methods toward the prediction and calculation, in the design stage and in service, of the strength and load characteristics of the layers of multilayer composite coatings and systems of the type of "chromium carbide–oxide ceramics–aluminum or its alloy" and "oxide ceramics–aluminum–polymer–steel base."

We propose multi-element composite rheological models and a method for calculating the strength and load characteristics of multilayer composite coatings based on them. These models make it possible to establish a correlation between the structural-mechanical properties (elasticity, viscosity, plasticity), the physicochemical structure, and the design of a composite system, as well as to evaluate their strength and load characteristics in the design stage of bearing assemblies and sliding bearings and increase the accuracy of predicting stress-deformation states of coatings under different loading conditions.

The experimental check by comparing the calculated and experimental data has corroborated the adequacy of the developed models and computational procedure.

It has been found that in the case of localized loading the admissible specific contact pressures for the "aluminum alloy–oxide ceramics–chromium carbide" system are 3 to 3.5 GPa and for the composite system including polymer layers — 1 to 1.5 GPa. The load-carrying capacity and the rheological behavior of the investigated systems based on oxide ceramics depend on the physicomechanical properties, the scheme of alternation of coating layers, and their thicknesses.

NOTATION

ε, composite system deformation, m; σ, stress, Pa; E, elastic modulus of material, Pa; η, viscosity coefficient, N/(m·sec); μ, Poisson coefficient; C, constant of integration; R, indenter radius, m; D, discriminant; V, rate of hardness indentation, N/sec; t, time, sec; φ, S, k, ψ, β, A, B, K, F, M, coefficients; τ, time interval between t_0 and t_1, sec; α_{ind}, indentation depth, m; P, load, N; L, dent profile length, m. Subscripts: 1 and 2, elements of rheological models 1 and 2, respectively; 21 and 22, elastic elements 1 and 2 of the rheological model 2; 0, initial instant of time t_0; unl, unloading; ind, indentation; *, derivative of equation; x and y, compression and tensile stresses.

REFERENCES

1. H. R. Hertz, *Hertz's Miscellaneous Papers*, Chs. 5 and 6, Macmillan, London (1896).
2. M. Kireitseu, M. Istomin, and V. Basenyuk, in: Dr. Lesurer (ed.), *Proc. 2001 TMS Fall Meeting "Modeling the Performance of Engineering Structural Materials II,"* USA (2001), pp. 355–364.
3. M. Kireitseu and V. Basenyuk, in: Dr. Lesurer (ed.), *Proc. 2001 TMS Fall Meeting "Modeling the Performance of Engineering Structural Materials II,"* USA (2001), pp. 365–377.
4. B. Latella, *J. Am. Ceram. Soc.*, **80**, No. 4, 1027–1031 (1997).
5. T. Yoshioka, T. Kitahara, and T. Yuine, *Wear*, **133**, No. 2, 373–383 (1989).
6. V. V. Bakovets and O. V. Polyakov, *Plasma-Electrolyte Anode Processing of Metals* [in Russian], Novosibirsk (1991).
7. V. N. Malyshev, V. V. Bakovets, and O. V. Polyakov, *Fiz. Khim. Obrab. Mater.*, No. 1, 82–87 (1985).
8. G. A. Markov, *Vestn. MGTU, Ser. Mashinostroenie*, No. 1, 14–21 (1992).
9. V. L. Basinyuk, M. L. Kireitsev, N. P. Chernyuk, and I. A. Yakimovich, in: *Coll. of Sci. Papers Presented at Int. Sci.-Eng. Conf. "Strengthening, Recovery, and Repair"* [in Russian], Novopolotsk (2001), pp. 348–352.
10. V. L. Basinyuk, M. L. Kireitsev, and M. A. Belotserkovskii, in: *Coll. of Sci. Papers Presented at Int. Sci.-Eng. Conf. "Strengthening, Recovery, and Repair"* [in Russian], Novopolotsk (2001), pp. 110–113.
11. RF Patent No. 20.356, MPK F 16 H 1/48.
12. RF Patent No. 20 352, MPK F 16 C 17/08.
13. RF Patent No. 2.175.686, MPK C 23 C 28/00.
14. V. Basenyuk and M. Kireitsev (Kireytsev), in: *Proc. Symp. of Material and Construction Failure*, Augustov, Poland (2001), p. 14.
15. V. Basenyuk, M. Kireitsev (Kireytsev), and A. Fedaravichus, in: *Proc. Symp. of Material and Construction Failure*, Augustov, Poland (2001), p. 12.
16. Z. P. Shul'man and É. A. Zal'tsgendler, *Rheophysics of Conglomerate Materials* [in Russian], Minsk (1977).
17. K. L. Johnson, *Contact Mechanics* [Russian translation], Moscow (1989).
18. B. R. Lawn, N. P. Padture, H. Cai, et al., *Science*, **263**, 1114–1116 (1994).
19. B. R. Lawn, *J. Am. Ceram. Soc.*, **81**, No. 9, 2394–2404 (1998).
20. B. R. Lawn, N. P. Padture, F. Guiberteau, and H. Cai, *Acta Metal Mater.*, **42**, No. 5, 1683–1693 (1994).